

Medium effects on the electro-deposition of MnO₂ on glassy carbon electrode

A comparative study in alkane, perfluoro alkane carboxylic acids and methanesulphonic acid

A. Manivel, N. Ilayaraja, D. Velayutham, M. Noel*

Central Electrochemical Research Institute, Karaikudi-630 006, Tamilnadu, India

Received 17 December 2006; received in revised form 22 March 2007; accepted 4 June 2007

Available online 12 June 2007

Abstract

Voltammetric studies of Mn(II) were carried out in acetic acid (AA), trifluoroacetic acid (TFA), butyric acid (BA), perfluorobutyric acid (PFBA) and methanesulphonic acid (MSA) media. Influence of anodic limit and the nature of acids were investigated. Oxidation of Mn(II) shows two anodic peaks in weak acids namely acetic acid and butyric acid media due to the formation of insoluble Mn(III) and Mn(IV) species. Reduction of these species were also observed as two peaks in the cathodic region. Formation and reduction of solid oxide phases are the dominant electrode processes in such weak acid media. In strong acids like MSA and TFA media sharp anodic and cathodic peaks were obtained due to the formation and reduction of stable soluble Mn(III) species. SEM studies reveal the formation of thicker oxide phases in weak acid media and much thinner oxide layers in strong acid media. γ -MnO₂ phase was formed from AA and TFA while ϵ -MnO₂ phase was formed from BA and PFBA, suggesting a relationship between phase structure and anionic size.

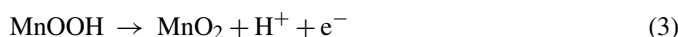
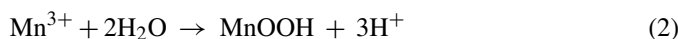
© 2007 Elsevier Ltd. All rights reserved.

Keywords: Cyclic voltammetry; Manganous oxidation; Acetic acid; Trifluoroacetic acid; Butyric acid; Perfluorobutyric acid

1. Introduction

Electro-deposition of MnO₂ is receiving greater attention in recent times from the point of view of preparation of high surface area nano wires and nano tubes [1], nano structured electrochemical capacitors [2], battery electrodes [3], electrocatalytic electrode for oxygen reduction [4] and development of MnO₂-based sensors for carbohydrates [5]. Generally γ -variety of MnO₂ is formed on platinum electrode in hot sulphuric acid medium [6–9]. The Mn(II) oxidation to MnO₂ proceeds either through ECE or disproportionation mechanism [10].

ECE mechanism



Disproportionation mechanism



SEM study [11] and XRD techniques [12] are commonly employed for the structural characterization of electro-deposited MnO₂. In general γ -MnO₂ and ϵ -MnO₂, which differ only in the level of microtwinning defects, are obtained during electro-deposition [13]. Electro-deposition of MnO₂ on gold electrodes has also been reported recently [14]. As cited above the electro-deposition of MnO₂ is generally carried out in hot H₂SO₄.

The Mn(III) species can be stabilized by choosing appropriate electrolyte and acid strength [15,16]. In phosphoric acid [15], pyrophosphoric acid [17] and strong methanesulphonic acid [16], Mn(III) species exhibit relative stability. Based on cyclic voltammetric study alone Nijjer et al. have concluded that MnO₂ formation is favoured at low pH and acid strength [18]. Relatively weak acidic acetic acid leads to formation of

* Corresponding author. Fax: +91 4565227779/91 4565227713.

E-mail address: yemenoel@yahoo.co.in (M. Noel).

γ -MnO₂ [19]. MnO₂ electro-deposited at low temperature exhibit poor adherence [8] and poor crystallinity [20]. MnO₂ may be further oxidized to MnO₄⁻ in the presence of Bi(V) cations [21]. Fe(II) ions also influence the electro-deposition as well as the electro-reduction of MnO₂ [22].

In the present work the influence of acidity and anionic species, which can act as a ligand in stabilizing the Mn(II) and Mn(III) ionic species on the electro-deposition of MnO₂ on glassy carbon surface is reported. Acetic acid (AA), trifluoroacetic acid (TFA), butyric acid (BA), perfluorobutyric acid (PFBA) and methanesulphonic acid (MSA) were employed as electrolytes. Perfluorocarboxylic acids exhibit stronger acidity when compared to the corresponding alkane carboxylic acids. For example, TFA and AA have similar molecular structure while their acidity differs substantially. This is also true for BA and PFBA. The influences of all these four acids on the electro-deposition of MnO₂ are investigated using cyclic voltammetry. The morphology of the electro-deposits and its crystalline nature are also characterized using scanning electron microscope (SEM) and X-ray diffraction (XRD), respectively. For comparative purposes the electro-deposition process in MSA [16] is also discussed.

2. Experimental

A 5 mm diameter glassy carbon (GC) working electrode, platinum counter electrode and standard calomel reference electrode (SCE) assembled in an undivided cell were used for cyclic voltammetry as well as preparation of electro-deposited MnO₂ samples. The GC working electrode was electrochemically pretreated whenever necessary according to known procedure [23]. The electrode activity was frequently evaluated by ferricyanide/ferricyanide redox system [23]. The stock solutions of required Mn(II) concentration were prepared by dissolving MnCO₃ directly in the required acid to eliminate the presence of any other interfering ionic species. The solid MnCO₃ was first mixed with 2 mol equivalent of the corresponding acid; the resultant solution was made up to required volume using 2.0 M acid. PFBA was prepared by electrochemical perfluorination process in this laboratory and distilled before use. All other acids and chemicals used were of analytical grade. Triple distilled water was used through out the experiments. All the experiments were carried out at room temperature (25 ± 2 °C).

Scanning electron microscopic images were recorded using JEOL JSM-35CF instrument, and XRD patterns of electro-deposited MnO₂ samples were recorded using X'pert Pro PANalytical (pw3040/60 X'pert PRO) at 40 kV and 30 mA of Cu K α radiation.

3. Results and discussion

3.1. Cyclic voltammetric studies in acetic acid medium

Typical cyclic voltammograms recorded with different concentrations of Mn(II) in 2.0 M acetic acid (pH = 2.09) are presented in Fig. 1. The background voltammogram recorded

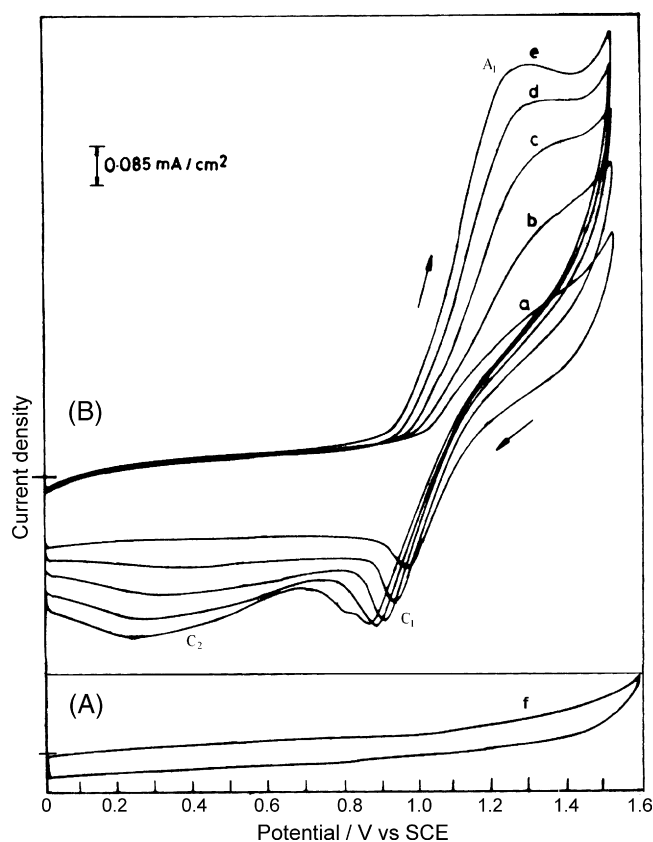


Fig. 1. Cyclic voltammograms of Mn(II) acetate; (A). Mn(II) free 2.0 M acetic acid; (B). Mn(II) in 2.0 M acetic acid under different concentrations of manganous acetate on GC electrode. Concentration of Mn(II) = 7.7, 14.8, 21.5, 27.6 and 33.3 mM from a–e respectively; Sweep rate = 40 mV s⁻¹.

in the absence of Mn(II) is also presented in Fig. 1f for comparison. The background current is very low in the absence of Mn(II) species. However, at low Mn(II) concentrations the anodic oxidation peak is not distinctly visible. With increasing concentration the anodic peak around 1.3 V becomes distinctly visible and separated from the background current which increases around 1.5 V. To ensure good electro-deposition without competitive background oxidation processes like oxygen evolution, the concentration of Mn(II) for all subsequent electro-deposition processes was chosen to be 33.3 mM (Fig. 1e). In the cathodic sweep, a sharp well defined peak C₁ is observed close to the oxidation potential region, which is followed by a much broader cathodic reduction wave C₂.

Effect of sweep rate on the voltammetric responses of 33.3 mM Mn(II) is presented in Fig. 2. All peaks are found to increase with increasing sweep rates. The anodic peak in A₁ region and the cathodic peak in the C₁ region are found to split into two closely spaced peaks in these voltammograms. The anodic peaks have been attributed to two distinct oxidation mechanisms represented by Eqs. (1)–(6) in the literature. The cathodic peak in the C₁ region is attributed to the reduction of MnO₂ to MnOOH, which is further reduced to Mn(II) in the C₂ potential region. A further insight, into the nature of the electro-oxidation as well as reduction processes are provided through more results reported here.

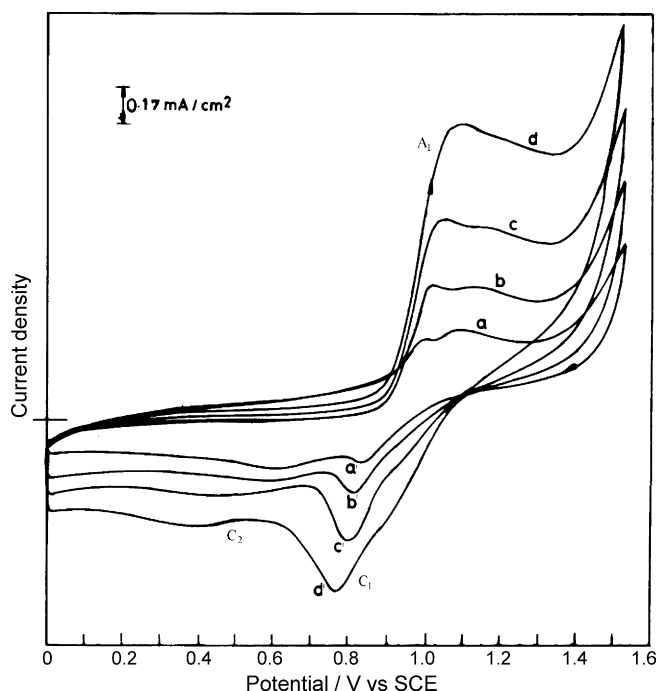


Fig. 2. Cyclic voltammograms of Mn(II) acetate in 2.0 M acetic acid at different sweep rates on GC electrode. Concentration of Mn(II) = 33.3 mM; Sweep rate = 5, 10, 20 and 40 mV s⁻¹ from a–d respectively.

3.2. Multi-sweep cyclic voltammetric studies in different media

The electro-deposition and subsequent reduction behaviour of MnO₂ in all the five different acid media were compared by recording multi-sweep cyclic voltammograms under identical conditions at a slow sweep rate of 5 mV s⁻¹. These cyclic voltammograms for acetic acid, trifluoroacetic acid, methanesulphonic acid, butyric acid and perfluorobutyric acid are presented in Figs. 3–7, respectively.

The multi-sweep cyclic voltammograms recorded in acetic acid (Fig. 3) are different from those recorded in TFA (Fig. 4) in many significant ways (compare Fig. 3 and Fig. 4). In acetic acid the oxidation process begins around 0.9 V where as this process begins only beyond 1.2 V in TFA. In acetic acid the anodic oxidation current increases with increasing sweep number quite significantly. In the second and subsequent sweeps the MnO₂ growth proceeds around 1.0 V, increases substantially and is visible as a distinct new anodic peak. In TFA only one well-defined anodic peak, which increases with increase in sweep number is noticed (Fig. 4). However, during potential reversal anodic current values are observed to be higher than the forward current values. This type of current cross over is generally due to further growth of deposits on the previously nucleated MnO₂ layers.

In a relatively weak acetic acid medium, Mn(III) species generated can undergo facile hydrolysis leading to MnOOH formation Eq. (2). These adsorbed MnOOH layers can facilitate further oxidation and MnO₂ film growth at lower potential regions (around 1.0 V). Hence, relatively little nucleation over-voltage is required in acetic acid medium. Two anodic oxidation

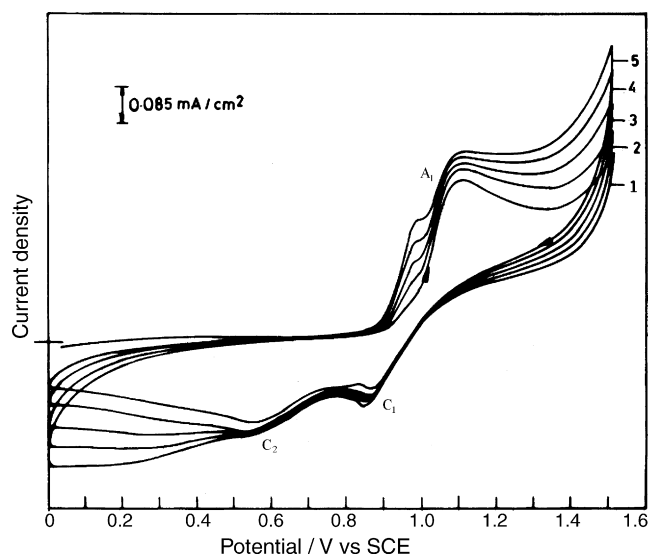


Fig. 3. Multi-sweep voltammograms of Mn(II) acetate in 2.0 M acetic acid on GC electrode. Concentration of Mn(II) = 33.3 mM; Sweep rate = 5 mV s⁻¹. 1–5 denote first five cycles.

peaks may correspond to distinct oxidation steps of Mn(II) and Mn(III) species (Eq. (1) and (3)) are transformations involving solid hydroxide or oxide phases.

In the strong TFA (pH = 0.70) medium Mn(III) hydrolysis may be more difficult. In fact trifluoroacetate anion may act as a ligand forming stable Mn(III) complexes.



Hence, MnO₂ formation in this media is substantially lower and would require significant nucleation over voltage and hence the deposition starts at more positive region (Fig. 4). Stable Mn(III) complex is predominantly formed in this medium.

The cathodic reduction of MnO₂ formed in acetic acid and TFA also exhibit significant differences. In acetic acid the cathodic current C₁ region is substantially lower when compared to the same in TFA medium (compare Fig. 3 and Fig. 4). The reduction current in the C₂ region in acetic acid is substan-

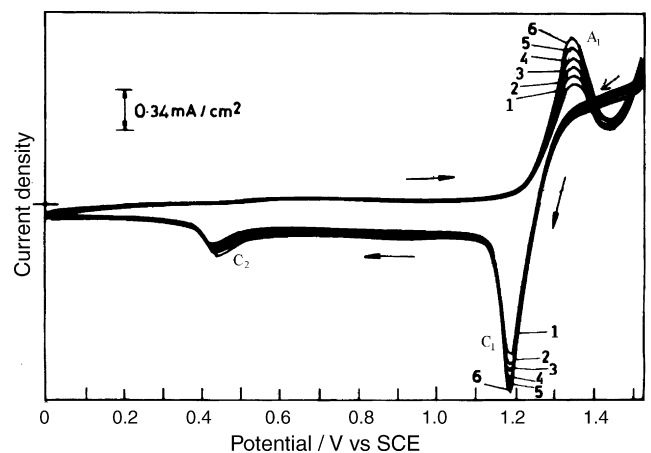


Fig. 4. Multi-sweep voltammograms of Mn(II) trifluoroacetate on GC electrode in 2.0 M TFA. Sweep rate = 5 mV s⁻¹. Concentration of Mn(II) = 33.3 mM. 1–6 denote first six cycles.

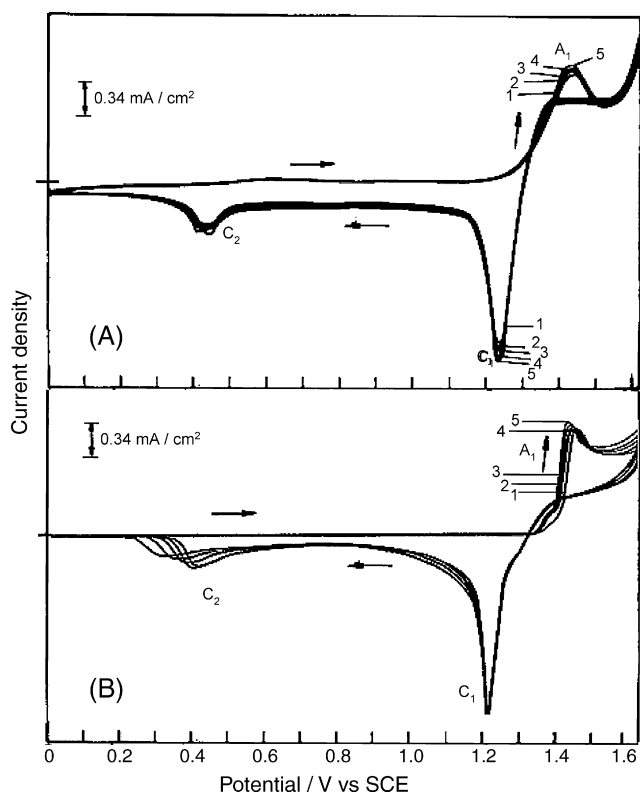


Fig. 5. Multi-sweep voltammograms of Mn(II) methanesulfonate (A) 2.0 M methanesulphonic acid on GC electrode. (B) 0.5 M methane sulphonic acid neutralized with 0.45 M NaOH. Concentration of Mn(II)=33.3 mM, sweep rate = 5 mV s⁻¹. 1–5 denote first five cycles.

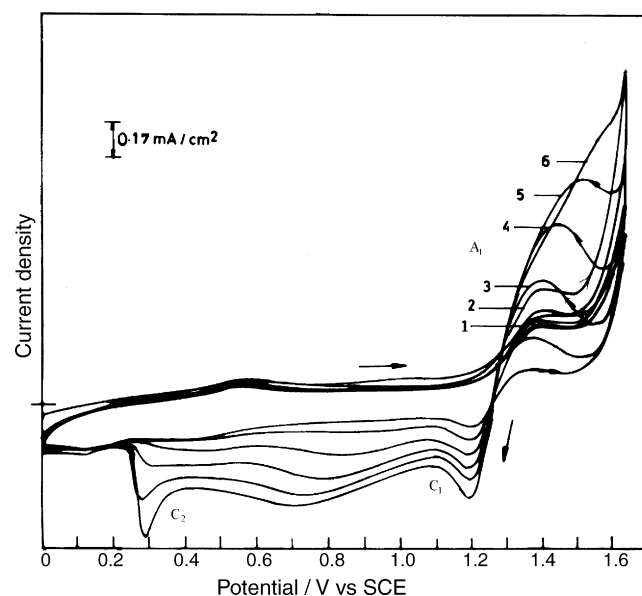
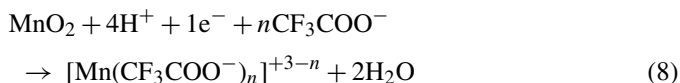


Fig. 7. Multi-sweep voltammograms of Mn(II) perfluorobutyrate in 2.0 M perfluorobutyric acid on GC. Concentration of Mn(II)=33.3 mM; Sweep rate = 5 mV s⁻¹; 1–6 denote first six cycles.

tially higher and also increases with increasing sweep number. In TFA the reduction current in the C₂ region is significantly smaller. This current does not increase with increasing sweep number.

It appears that the higher stability of the soluble Mn(III) complex species in TFA is once again responsible for the significant differences in the voltammetric behaviour in the cathodic region in acetic acid and TFA. In TFA, MnO₂ formed on the electrode surface is directly and substantially reduced to soluble Mn(III) species in the C₁ potential region.



In addition to this process, direct reduction of Mn(III) complex to Mn(II) species also probably occurs in the same C₁ potential region (reverse process of Eq. (7)). Only a small remaining portion of chemisorbed MnOOH species on the electrode surface undergoes further reduction in the C₂ region in TFA. In acetic acid, on other hand, the MnOOH species formed in the C₁ region prevents further reduction of MnO₂ species in the interior of the electrode surface hence the reduction of the MnO₂ layer occurs over a much broader potential range.

The above conclusion was also supported by physical verification of the glassy carbon surface after each multi-sweep cycling experiment. Presence of fairly thick MnO₂ oxide layer was visible to the naked eye on glassy carbon surface cycled in acetic acid under experimental condition described in Fig. 3. In contrast, the glassy carbon surface after potential cycling in TFA was fairly bright and clean. To further verify the influence of acid strength on Mn(II) oxidation, the cyclic voltammetric responses on the another strong acid, namely methanesulfonic acid, were also recorded.

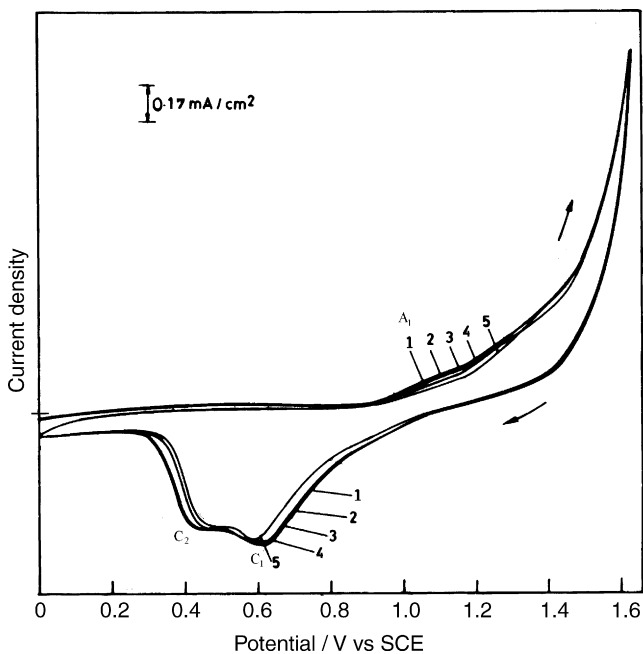


Fig. 6. Multi-sweep voltammograms of Mn(II) butyrate in 2.0 M butyric acid on GC electrode. Concentration of Mn(II)=33.3 mM; Sweep rate = 5 mV s⁻¹, 1–6 denote first six cycles.

The multi-sweep cyclic voltammograms for Mn(II) oxidation recorded in methanesulphonic acid (Fig. 5) is quite similar to those recorded in TFA (compare Fig. 4 and Fig. 5). Methanesulphonic acid is also a strong acid and the methane sulphonate anion also can form stable soluble Mn(III) complexes as TFA and hence good similarity in the electro-deposition and subsequent reduction behaviour of MnO_2 in these two media. The higher stability of Mn(III) species in strong methanesulphonic acid (pH = 0.30) medium has already been reported from this laboratory [16]. The difference between cyclic voltammetric responses of strong and weak acids like acetic acid and trifluoroacetic acid may either be due to the change in pH or the change in the stability constants of the complexes formed. It would indeed be interesting to obtain stability constant for Mn(II) and Mn(III) species involving different anions investigated in this work, such data however are not available. However, a few cyclic voltammetric experiments were carried out in methanesulfonic acid keeping the concentration of CH_3SO_3^- anion at higher level and varying the pH between 0.3 and 2. Typical multi-sweep cyclic voltammograms recorded in 33.3 mM Mn(II) species in 0.5 M MSA neutralized by 0.45 M NaOH (pH = 1.2) are shown

in Fig. 5B. The similarity between Fig. 5A and Fig. 5B are apparent despite significant variation in pH. This suggested that the complexing ability of the anionic species is much more important when compared to pH variations encountered in the present work (pH = 0.3–2.8).

The multi-sweep cyclic voltammetric responses of Mn(II) in BA (pH = 2.8) and PFBA (pH = 0.69) once again significantly different from each other. The anodic oxidation once again starts around 0.9 V in butyric acid (Fig. 6). The oxidation processes occur as a broad wave. During cathodic reduction, the C_1 and C_2 regions merge together at more negative potentials. Fairly thick and visible oxide layer is noticed after multi-sweep cycling in this medium. The MnO_2 oxide layer formed in this medium probably undergoes predominantly solid-state reduction to MnOOH phases. Butyrate anion is too large to exhibit a stabilizing influence and solublize the Mn(III) species.

Perfluorobutyric acid is relatively strong acid and hence electro-deposition of MnO_2 occurs through nucleation growth processes as indicated in the multi-sweep voltammograms presented by Fig. 7. In this respect, the electro-deposition process

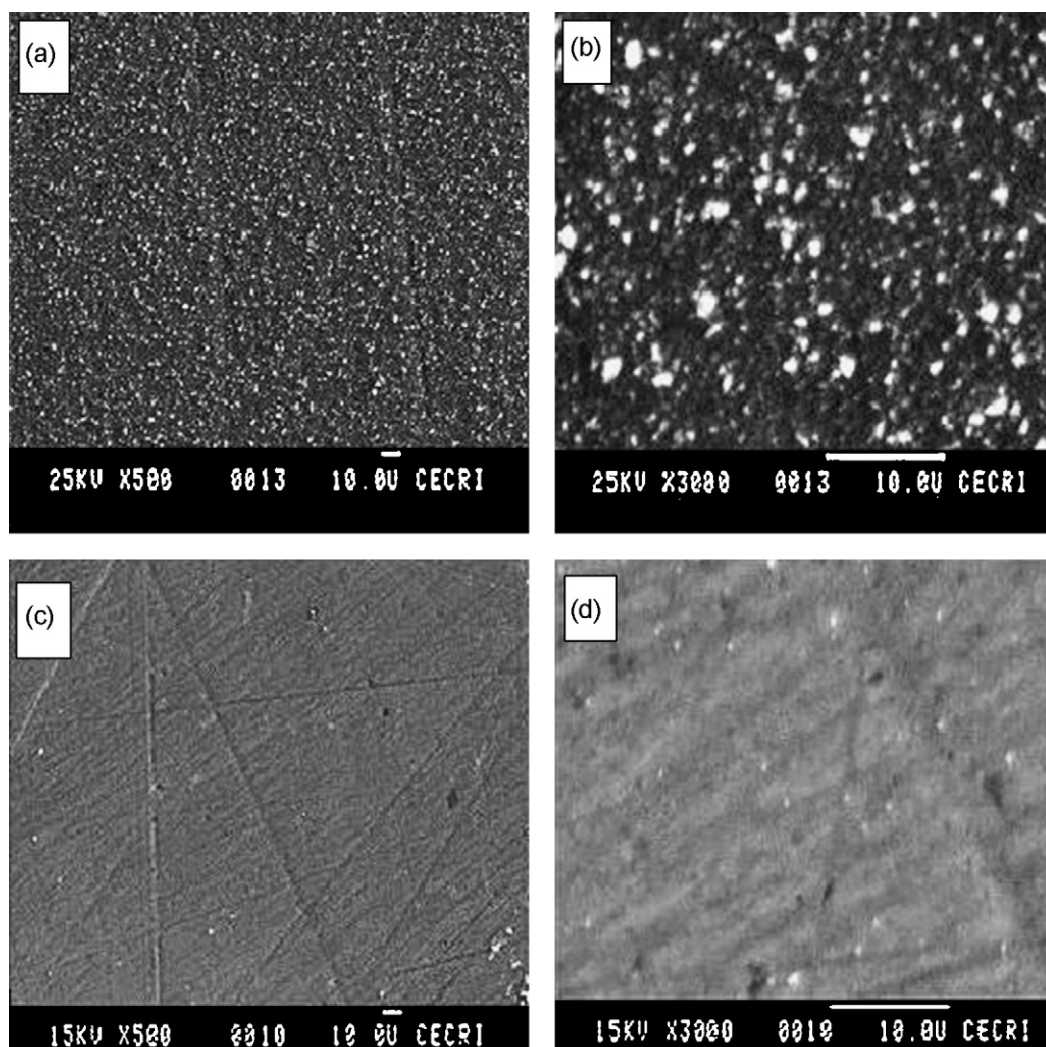


Fig. 8. SEM images of deposits obtained in 33.3 mM Mn(II) (a) acetic acid-X500, (b) acetic acid –X3000, (c) TFA-X500 and (d) TFA-X3000.

in PFBA and TFA are quite similar. However, perfluorobutyrate anion is also too large to form complexes with Mn(III) species, hence the MnO_2 formed in A_1 region is reduced only to a small extent in C_1 region. Hence, with each potential cycling more thickening of the oxide layer occurs as indicated by increasing anodic as well as cathodic currents with increasing sweep numbers.

It is apparent from the above comparative voltammetric study that both acidity and ligand forming capability of the anionic species contribute significantly towards the electro-deposition and reduction behaviour of MnO_2 . Stronger acids generally require higher nucleation over-voltage as in the case of TFA, MSA and PFBA. Anionic size and ligand forming capability determines the reductive dissolution of MnO_2 and film growth properties. TFA and MSA alone exhibit capability of forming and stabilizing Mn(III) complexes.

3.3. Morphology and crystalline structure of MnO_2 deposits

For characterization of MnO_2 deposited from four carboxylic acid media, electro-deposition was carried out by potential

cycling in anodic deposition region. Five potential cycles were carried out at 5 mV s^{-1} in all four cases.

The initial and final anodic deposition limits chosen for acetic acid and butyric acid from cyclic voltammetric data were 0.9 V and 1.1 V, respectively. For TFA and PFBA these limits were 1.2 V and 1.4 V, respectively. The electro-deposition was stopped at the higher anodic limit during the final cycle, thus preventing significant dissolution of the oxide formed.

Typical SEM photographs obtained for MnO_2 deposited on glassy carbon surface in acetic acid medium are presented in Fig. 8a and b, respectively. The electro-deposits were found to be thick and the particles were uniformly distributed. Fig. 8b indicates that the average particle size is in the range of $1 \mu\text{m}$ or less. The electro-deposits formed from TFA were found to be relatively thin (Fig. 8c and Fig. 8d). The polished glassy carbon substrate is clearly visible in these micrographs. It indicates that the electro-deposited MnOOH phase undergoes chemical dissolution in TFA as indicated by Eq. (8).

The SEM data obtained after electro-deposition in butyric acid also indicate uniform and thick film formation. The film formed is quite uniform. Occasionally, however some film rupture and peeling off occurs which indicates the nature of the

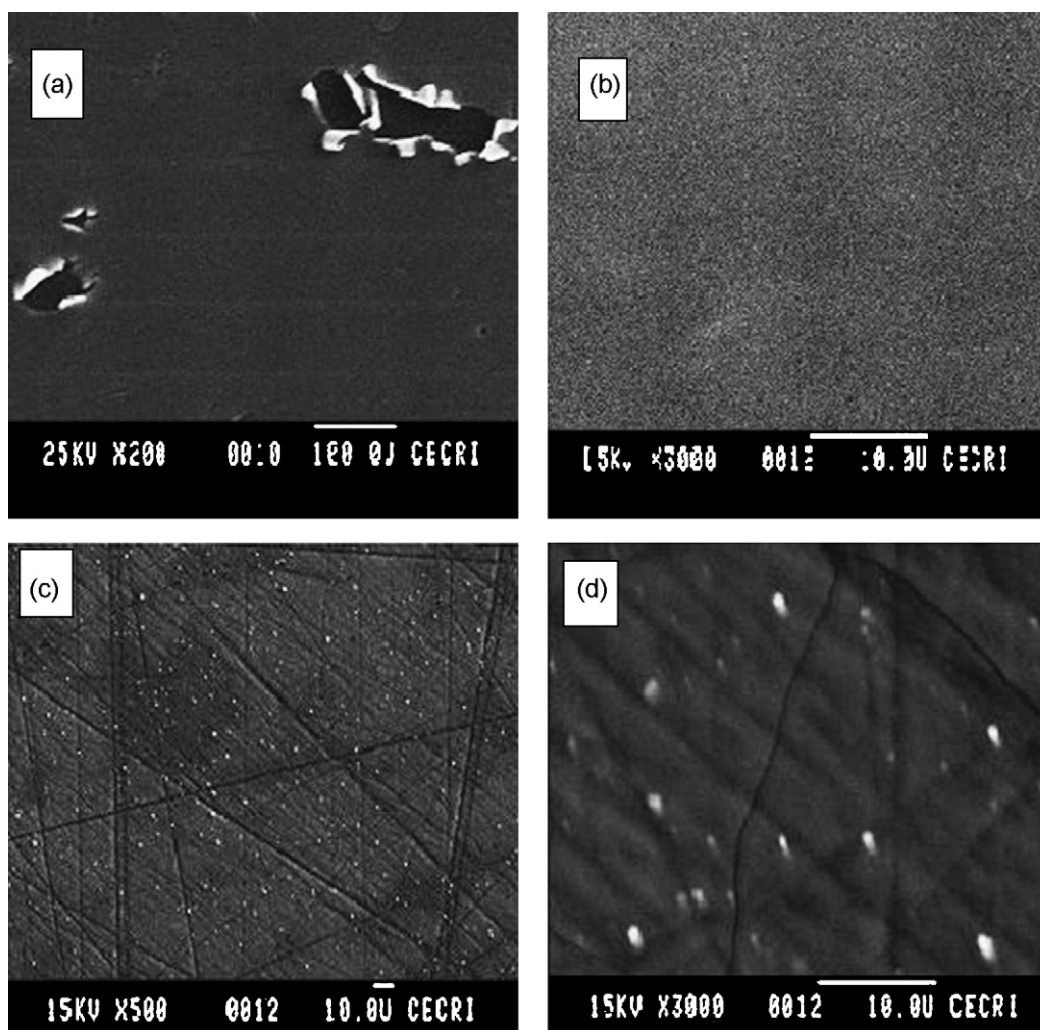


Fig. 9. SEM images of deposits obtained in 33.3 mM Mn(II) (a) butyric acid-X200, (b) butyric acid-X3000, (c) PFBA-X500 and (d) PFBA-X3000.

deposit forms (Fig. 9a). The uniformity of the deposit in non-rupture region is also indicated in Fig. 9b. Reasonably thin electro-deposits were also obtained from PFBA (Fig. 9c and Fig. 9d). The electro-deposits in PFBA (Fig. 9c and Fig. 9d) however, are once again thinner than those obtained in butyric acid (Fig. 9a. and Fig. 9b).

The XRD data also indicate some interesting structural variations in the electro-deposited MnO_2 in different media. In general, the XRD signals in alkane carboxylic acids are more intense when compared to those obtained in perfluorocarboxylic acids (Fig. 10 and Fig. 11). The MnO_2 crystals are also polycrystalline in nature. However, close comparison suggests similarity in the XRD patterns obtained for MnO_2 from acetic acid and TFA, on the one hand, (Fig. 10) and butyric acid and PFBA, on the other hand. Comparison of XRD peaks of maximum intensity with the data from JCPDS card (no.: 14-0644, 04-0779, 18-0805) suggests that MnO_2 deposits from acetic acid and TFA is dominated by γ -phase (Fig. 10). The MnO_2 deposits obtained from butyric acid and PFBA is (JCPDS card no.: 12-0141, 30-0820) dominated by ϵ -phase. The C–F bond length (1.324 Å) is quite similar to C–H (1.113 Å) bond length [24]. Hence, the structure of CH_3COO^- and CF_3COO^- would also be similar. Thus, both the anionic species influence the crystalline structure identically leading to electro-deposition of MnO_2 in both cases. The relatively larger sized $\text{C}_4\text{H}_9\text{COO}^-$ and $\text{C}_4\text{F}_9\text{COO}^-$ anions appeared to possess a microtwinning effect during electro-deposition leading to the formation of ϵ - MnO_2 .

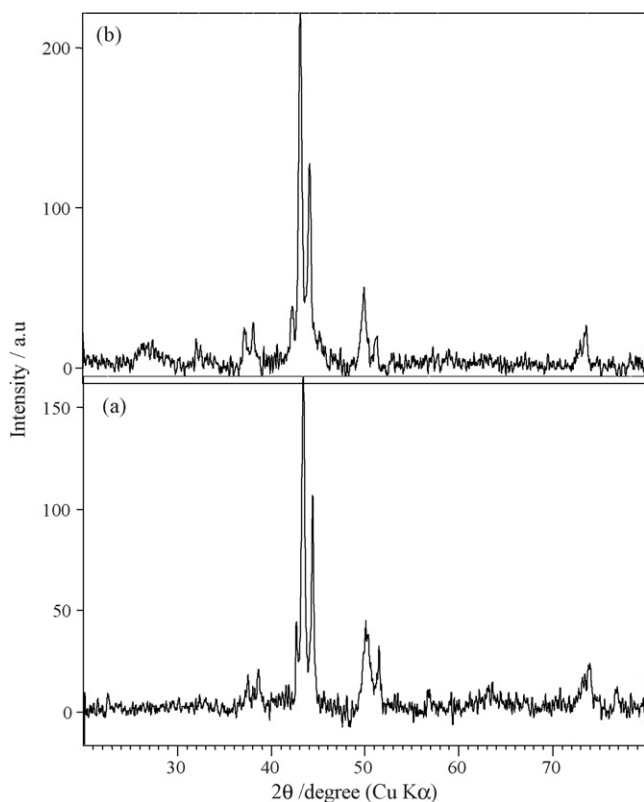


Fig. 10. XRD patterns of deposit obtained from 33.3 mM Mn(II) in (a) acetic acid and (b) TFA medium (compared with JCPDS no.: γ - MnO_2 -14-0644, 04-0779, γ - MnOOH -18-0805).

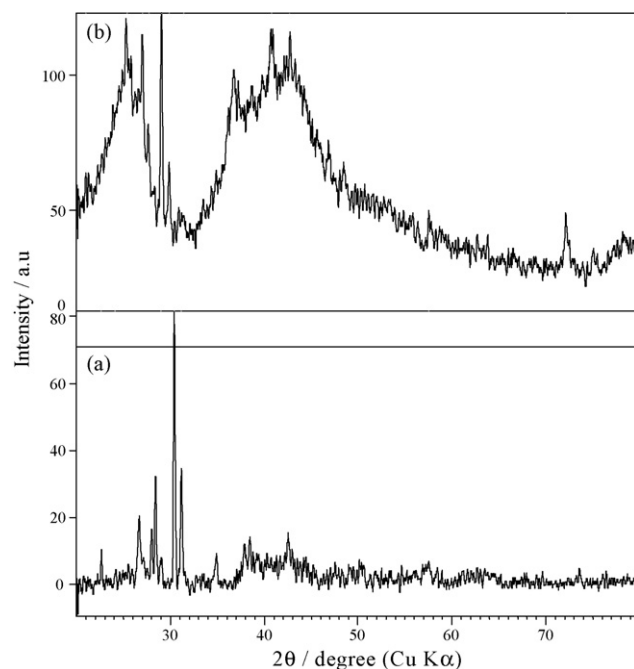


Fig. 11. XRD patterns of deposit obtained from 33.3 mM Mn(II) in (a) butyric acid and (b) perfluorobutyric acid medium (compared with JCPDS no.: ϵ - MnO_2 -12-0141, 30-0820).

4. Conclusions

The present investigation indeed suggests that the electro-deposition and dissolution behaviour of MnO_2 can significantly depend on the acidity as well as complexing ability of the ligands present in the electrolyte medium. Electro-deposition from strong acids would require significantly higher over-voltage. If the anionic species can complex and stabilize the Mn(III) species, sharp reduction/dissolution of electro-deposited MnO_2 can be achieved. Such media like TFA, MSA may be suitable for cathodic stripping voltammetric determination of trace level Mn(II) species. The medium may also influence the predominant type of MnO_2 crystals formed on the electrode surfaces. Further investigations on the possibilities of selectively forming nano particles of MnO_2 with different crystalline phases and their potential applications would be worthwhile.

Acknowledgements

The authors wish to acknowledge the Ministry of Environment and Forests, Government of India and CSIR, New Delhi, for financial support.

References

- [1] X. Wang, Y. Li, *Chem. Eur. J.* 1 (2003) 9.
- [2] S. Devaraj, N. Munichandraiah, *Electrochem. Solid State Lett.* 8 (2005) A373.
- [3] S. Devaraj, N. Munichandraiah, *J. Electrochem. Soc.* 154 (2007) A80.
- [4] M.S. El-Deab, T. Ohsaka, *J. Electrochem. Soc.* 153 (2006) A1365.
- [5] D. Das, P.K. Sen, K. Das, *J. Appl. Electrochem.* 36 (2006) 685.
- [6] E. Preisler, *J. Appl. Electrochem.* 6 (1976) 301.

- [7] S. Rodrigues, N. Munichandriah, A.K. Shukla, *J. Appl. Electrochem.* 28 (1998) 1225.
- [8] W.H. Kao, V.J. Weibel, *J. Appl. Electrochem.* 22 (1992) 983.
- [9] J.A. Lee, W.C. Maskell, F.L. Tye, *J. Electroanal. Chem.* 110 (1980) 145.
- [10] J.Ph. Pitiptierre, Ch. Comminellis, E. Plattner, *Electrochim. Acta* 35 (1990) 281.
- [11] K. Matsuki, T. Endo, H. Kamada, *Electrochim. Acta* 29 (1984) 983.
- [12] C.-H. Kima, Z. Akasea, L. Zhanga, A.H. Heuera, A.E. Newmanb, P.J. Hughesc, *J. Solid State Chem.* 179 (2006) 753.
- [13] Y. Chabre, J. Parmetier, *Prog. Solid State Chem.* 23 (1) (1995).
- [14] Z. Rogulski, H. Siwek, I. Paleska, A. Czerwinski, *J. Electroanal. Chem.* 543 (2003) 175.
- [15] D. Velayutham, M. Noel, S. Chidambram, *Bull. Electrochem.* 9 (1993) 99.
- [16] V. Devadoss, M. Noel, K. Jayaraman, C. Ahmed Basha, *J. Appl. Electrochem.* 33 (2003) 319.
- [17] J.A. Lee, W.C. Maskell, F.L. Tye, *J. Appl. Electrochem.* 79 (1977) 79.
- [18] S. Nijjer, J. Thonstad, G.M. Haarberg, *Electrochim. Acta* 46 (2000) 395.
- [19] J.N. Broughton, M.J. Brett, *Electrochim. Acta* 50 (2005) 4814.
- [20] S. Bodoardo, J. Brenet, M. Maja, P. Spinelli, *Electrochim. Acta* 39 (1994) 1999.
- [21] J. Lee, Y. Einaga, A. Fujishima, S.M. Park, *J. Electrochem. Soc.* 151 (2004) E265.
- [22] A.S. Pilla, M.M.E. Duarte, C.E. Mayer, *J. Electroanal. Chem.* 569 (2004) 7.
- [23] M. Noel, P.N. Anantharaman, *Analyst* 110 (1985) 1095.
- [24] P. Kirsch (Ed.), *Modern Fluoroorganic Chemistry, Synthesis, Reactivity and Application*, WILEY-VCH, Weinheim, 2004, p. p.9.